

**Article type:** Full length

**Running head:** Scleroderma microenvironment activates MSCs

**Title:** Pathogenic Activation of Mesenchymal Stem Cells is induced by the Disease Microenvironment in Systemic Sclerosis

**Authors:** Zeinab Taki PhD<sup>1</sup>, Elena Gostjeva PhD<sup>2</sup>, William Thilly ScD<sup>2</sup>, Bodoor Yaseen MSc<sup>1</sup>, Henry Lopez PhD<sup>1,3</sup>, Maria Mirza MB BS<sup>1</sup>, Zainab Hassuji MB BChir<sup>1</sup>, Shivane Vigneswaran MB BS<sup>1</sup>, Bahja Ahmed Abdi BSc<sup>1</sup>, Amy Hart BSc<sup>1</sup>, Nikita Arumalla MB BS<sup>1</sup>, Gemma Thomas BSc<sup>1</sup>, Christopher P Denton FRCP PhD<sup>1</sup>, Yasir Suleman MB BS<sup>1</sup>, Huan Liu PhD<sup>1,4</sup>, Cristina Venturini PhD<sup>5</sup>, Steven O'Reilly PhD<sup>6</sup>, Shiwen Xu PhD<sup>1</sup>, Richard Stratton MD PhD<sup>1</sup>

<sup>1</sup>UCL Centre for Rheumatology and Connective Tissue Diseases, Royal Free Hospital Campus, University College London Medical School, Rowland Hill Street, London, NW3 2PF, UK.

<sup>2</sup>Department of Biological Engineering, Massachusetts Institute of Technology Cambridge, MA, USA, <sup>3</sup>MuriGenics, Inc., 941 Railroad Avenue, Vallejo, CA, 94592, USA. <sup>4</sup>School of Public Health, Health Science Center, Xi'an Jiaotong University, Xi'an, Shaanxi 710061, PR China. <sup>5</sup>Pathogen Genomics Unit, University College London, London WC1E 6BT, <sup>6</sup>Department of Health and Life Sciences, Northumbria University, Newcastle Upon Tyne, NE1 8ST, UK.

**Corresponding author:** Richard Stratton, UCL Centre for Rheumatology and Connective Tissue Diseases, UCL Medical School, Royal Free Hospital Campus, Rowland Hill Street, London NW3. 2PF, [r.stratton@ucl.ac.uk](mailto:r.stratton@ucl.ac.uk), Tel: +44207 794 0500 x 33735.

**Funding:** The Rosetrees Trust, The Royal Free Charity, Arthritis Research UK.

**Author disclosures:** The authors have no relevant disclosures.

## **Abstract**

**Objective** In systemic sclerosis (SSc) a persistent tissue repair process leads to progressive fibrosis of the skin and internal organs. The role of mesenchymal stem cells (MSCs), which characteristically initiate and regulate tissue repair, has not been fully evaluated. We sought to investigate whether dividing metakaryotic MSCs are present in SSc skin, and test whether exposure to the disease microenvironment activates MSCs leading to transdifferentiation.

**Methods** Skin biopsy material from recent onset diffuse SSc patients was examined by collagenase spread of 1mm thick surface-parallel sections, in order to identify metakaryotic dividing stem cells in each tissue plane. Adipose-derived MSCs from healthy controls were treated with dermal blister fluid from diffuse SSc patients, and profiled by next generation sequencing, or evaluated for phenotypic changes relevant to SSc. Differential responses of dermal fibroblasts were studied in parallel.

**Results** MSC-like cells undergoing active metakaryotic division were identified in SSc but not control sections, most prominent in the deep dermis and adjacent to damaged microvessels, in both involved and clinically uninvolved skin. Furthermore, exposure to SSc blister fluid caused selective MSC activation, inducing a myofibroblast signature, whilst reducing signatures of vascular repair and adipogenesis and enhancing migration and contractility. Microenvironment factors implicated in inducing transdifferentiation include the pro-fibrotic growth factor TGF $\beta$ , presence of lactate and mechanosensing, whereas the microenvironment Th2 cytokine IL-31, enhanced osteogenic commitment (calcinosis).

**Conclusion** Dividing MSC-like cells are present in the SSc disease microenvironment where multiple factors, likely acting in concert, promote transdifferentiation, leading to a complex and resistant disease state.

## Introduction

In scleroderma (systemic sclerosis, SSc), a prototypic disease for understanding fibrosis, infiltration of the affected tissues by dysregulated immune cells at the disease onset is followed by a persistent tissue repair process resulting in progressive fibrosis of the skin and internal organs (1). Within the early disease microenvironment cross-talk between immune cells and tissue resident cells is presumed responsible for promoting myofibroblast activation, leading to increased extracellular matrix (ECM) production, and progression to scarring and fibrosis of the skin and internal organs (2). However, the exact mechanisms and cellular interactions involved, as well as the cellular origin of the activated myofibroblasts, are not fully understood, limiting the development of specific therapeutic approaches. Unlike other fibrotic disorders, in SSc the early disease microenvironment can be readily sampled using a minimally invasive technique to obtain lesional tissue fluid, allowing for the identification of candidate factors and modelling of the interaction with target cells (3).

Mesenchymal stem cells (MSCs) are tissue resident cells with multi-lineage potential which are involved in organogenesis but quiescent in healthy adult tissue (4, 5). However, following wounding or tissue damage MSCs become activated, divide and orchestrate tissue repair (6). MSCs are implicated as having a role in fibrosis, since their activation can account for the excessive tissue remodeling seen (7). The role of MSCs in SSc has not been fully explored, but their involvement in SSc could account for several disease manifestations, most prominently the fibrosis, but also dysregulated vascular repair and ectopic bone formation (calcinosis)(8, 9). Furthermore, depletion of MSCs through multiple cycles of activation and division in SSc tissues could explain tissue atrophy, loss of subcutaneous fat and non-healing wounds seen in late stage disease (10).

In this study, we investigate local activation of MSCs in SSc skin lesions, using a novel histologic method to detect metakaryotic dividing cells (11). Furthermore, we use treatment of cultured adipose derived MSCs with SSc lesional tissue fluid, combined with next generation sequencing (NGS), to comprehensively model the interaction between the early disease microenvironment and MSCs and go on to investigate the role of individual candidate factors present in the disease tissue.

## **Patients and Methods**

### *Patient samples*

All patients had a definite diagnosis of SSc according to the 2013 ACR/EULAR SSc classification criteria (12). All human studies were carried out in compliance with the declaration of Helsinki. SSc patients from the diffuse cutaneous subset within the first 2 years of disease, were selected for blister fluid (BF) sampling. Using a dermal suction apparatus (Electronic Diversities, MD, USA) and a technique originally devised by Sondergaard et al, an 8mm blister was formed on the anterior forearm of patients and healthy controls under negative pressure (280-310 mmHg) over 3 hours(13). The interstitial fluid in the blister was aspirated using a 23-gauge needle. 100-250  $\mu$ l of fluid is collected per blister and stored in 1.5 ml Eppendorf tubes following centrifugation at 4°C for 10 minutes and decantation of the supernatant. Samples were kept in 20  $\mu$ l aliquots at -80°C until needed, and then used in tissue culture diluted 1 in 125 in DMEM with 0.2%FCS. The L-lactate Colorimetric Assay (Biovision, CA, USA) was used to detect the amount of lactate in SSc and healthy control BF, IL-31 was assayed by ELISA (R&D systems, #DY2824), and TGF $\beta$  by ELISA (R&D Systems, Quantikine ELISA #DB100B).

### *Skin biopsy collection and metakaryotic staining*

Skin punch biopsies of 4mm diameter and 5mm depth were taken from the involved anterior forearm skin of 4 patients with recent onset diffuse SSc less than 2 years since the first non-Raynauds symptoms, and 4 healthy controls, after written informed consent (using a study specific consent form and patient information sheet). In further replicate studies, 4 further recent onset diffuse SSc patients were studied by biopsy of involved forearm skin and clinically uninvolved skin from the back. Biopsies were fixed in Carnoy's fixative (3 parts ethanol to 1-part glacial acetic acid), mixed immediately before adding the tissue. The biopsies were stored at 4°C with fixative being replaced three times, once every hour, before being stored long term in 70% ethanol at 4°C. Using a method developed by Dr Elena Gostjeva(14), tissues were assessed for the presence of metakaryotic stem cells. Biopsies were cut laterally into three 1 mm sections using a scalpel and each piece digested in collagenase II (0.8mg/ml) at 37°C for two hours. Sections were then placed in 1M HCL at 60°C for 8 minutes for hydrolysis to occur. Acid treatment

releases the aldehydes by cleavage of the N bases and formation of aldehyde groups to which Schiff's staining binds. Schiff's staining is DNA specific and staining intensity is proportional to DNA concentration (15). After hydrolysis, sections were rinsed in distilled H<sub>2</sub>O and placed into a Petri dish at room temperature containing 45% acetic acid for 15-30 minutes. Individual sections were placed on glass microscope slides and 5µl acetic acid pipetted on top before covering with a glass coverslip and spreading the section with slight pressure until a thin uniform layer was achieved. Slides were placed on dry ice until frozen, before immersion in Schiff's reagent for one hour, and then rinsed twice in 2 x saline-sodium citrate (SSC) buffer, once for 30 seconds, once quickly. Slides were then rinsed with distilled H<sub>2</sub>O and dipped in 1% Giemsa solution for 5 minutes before rinsing in Sorensen buffer and distilled H<sub>2</sub>O. Slides were allowed to dry fully before being immersed in xylene for 3 hours and mounting with DPX mountant. Slides were scanned with a LEICA SCN400F scanner. Quantification of metakaryotic nuclei was conducted by counting the number of bell-shaped nuclei in 10 randomly selected 20x magnification field views per slide and determining the average number of MSCs per section.

### *Culturing cells*

Human adipose-derived MSCs, isolated from liposuction fat, were obtained commercially (Adipose-Derived Mesenchymal Stem Cells; Normal, Human (ATCC, #PCS-500-011). These cells have been demonstrated to be multipotent, capable of differentiating down the adipogenic, osteogenic and chondrogenic lineages, and shown by FACS to be positive for CD29, CD44, CD73, CD90, CD105 and CD166, and negative for CD14, CD19, CD34 and CD45(16). DMEM supplemented with 20% serum and penicillin/streptomycin, was used to culture MSCs for three days in plastic T75 flasks (Corning; New York, USA), before replacing media with 10% serum. Negative controls were represented by DMEM supplemented with 0.2% serum. Where specified, MSCs were cultured in osteogenic (OIM) or adipogenic induction media (AM)(Gibco, UK) in N=4 replicates per experiment. Cells were trypsinised and passaged by incubation with Trypsin/EDTA (Life Technologies, Paisley, UK).

Primary cultures of normal skin fibroblasts were obtained from 4mm punch biopsies sampled from forearm skin of healthy controls. Biopsy material was minced and cultured in 20% serum. Cultures were inspected daily by light microscopy and when a fibroblast outgrowth was detected,

cells were washed with DPBS and contaminating epithelial cells were detached by Trypsin/EDTA. Fibroblasts were cultured further and then subcultured in T75 tissue culture flasks. Passaged cells were cultured further in DMEM supplemented with 10% FCS and penicillin/streptomycin solution, incubated at 37°C 5% CO<sub>2</sub> in T75 flasks. All fibroblasts were used at passage 3-5 for each experiments to correspond with MSC passage numbers and to avoid the effects of senescence.

#### *Protein and qPCR assays*

Cells were lysed in RIPA buffer then separated by SDS PAGE, and transferred to nitrocellulose blots which were probed with the following primary antibodies; CTGF (Santa Cruz, #sc14939), Collagen I (Abcam, #ab34710),  $\alpha$ SMA (Sigma, #a2547) and GAPDH (abcam, #ab8245), and then species specific secondary labelled antibodies developed with ECL. For qPCR analysis, RNA was extracted from lysed MSCs using Quiagen RNAeasy kit, and qPCR performed with the following primers TBP (used as reference gene) forward 5'-AGTGACCCAGCATCACTGTTT-3', reverse 5'-GGCAAACCAGAAACCCTTGC-3', CTGF forward 5'-GACCTGGAAGAGAACATTAAGAAGG-3', reverse 5'-TGAGTATGTCTTCATGCTGGTG -3', COL1A2 forward 5'-TGCTTGCAGTAACCTTATGCCTA-3', reverse 5'-CAGCAAAGTTCCACCGAGA-3',  $\alpha$ SMA forward 5'-CCGACCGAATGCAGAAGGA-3', reverse 5'-ACAGAGTATTTGCGCTCCGAA-3'.

#### *Next generation sequencing*

Analysis was conducted using 43 base paired end strands measuring 15 million reads per sample. The study was separated into two groups, one using healthy control dermal fibroblasts, and the other, adipose-derived MSCs, in order to compare the patterns of gene expression in SSc environment activated MSCs with those induced in fibroblasts. The RNAseq analyses was conducted in collaboration with UCL Genomics.

A heatmap was constructed using R software, based on the expression of 20 candidate genes, chosen for their potential relevance to SSc pathology, MSC differentiation capabilities or ability to induce pro-fibrotic factors. Pathway analysis was performed using Ingenuity Pathway Analysis (IPA) software to highlight predicted pathways involved, in the context of their physiological significance. This software uses the differentially expressed genes from the RNAseq data, inputted as FASTQ files, and with its own database called Knowledge Base, predicts the pathways activated or deactivation, networks of molecules involved and biological function by gene

ontology. These predictions are based on existing literature and experimental data. For the purpose of this study, only significantly changed RNA molecules were analysed where  $p < 0.05$ . IPA analysis compares two FASTQ files, and in this study, two comparisons were made; 0.2% media vs SSc blister fluid treated MSCs and, SSc blister fluid vs healthy control blister fluid treated MSCs. Significance was calculated by the software as  $-\text{Log}(p\text{-value})$ , and as such, all values above 1.3 were significant, indicating  $p < 0.05$ . Z-scores are computed by the software representing the level of matching between the predicted relationship direction (activation/deactivation) and the observed gene expression. A Z-score of  $>2$  or  $<-2$  is calculated as significant matching. Comparison was made with the results of Gene Ontology biologic process analysis in order to validate the IPA (<http://geneontology.org/>).

Furthermore, the software was used to predict networks of focus molecules, implicated in the responses of MSCs to SSc blister fluid. A score was algorithmically computed for each network based on the number of nodes, their significance and directionality. The score indicates the likelihood of connected nodes being generated by chance. A score of above 2 means that there is less than 1 in 100 chance of this. Nodes are either green or red, with green indicating activated by SSc blister fluid, and red, deactivation by blister fluid. The intensity of the colour of each node is a representation of the Z-score, i.e. the directionality of the connection, and how significant it is. Uncoloured, grey nodes are of molecules that were not found to be differentially expressed in the original RNAseq dataset and have been filled in by the software to complete the network. The shapes of the nodes represent the predicted function of that gene including enzymes, protein, receptors, kinases, cytokines, growth factors and transcription factors.

#### *Modelling stiff and soft ECM in the microenvironment*

ECM stiffness was modelled *in vitro* by culturing cells on Softwell collagen coated hydrogels of specific stiffness (Cell Guidance Systems SW12-COL-50, SW12-COL-4). 4 kPa and 50 KPa gels were used to model healthy and SSc skin, respectively. MSCs were seeded at a density of  $1 \times 10^5$  cells per well in N=4 replicate experiments, and incubated in DMEM supplemented with 10% serum, with media being changed every 3-4 days, being careful not to disrupt the hydrogel layer.

#### *Study approval*

Written informed consent was obtained from all patients and healthy controls under ethical committee approval, in compliance with the Helsinki Declaration. Ethical committee approval was obtained under “NHS Health Research Authority, NRES Committee London-Hampstead, HRA, reference number 6398- “Elucidating the pathogenesis of scleroderma”.

## **Results**

### *Presence of metakaryotic dividing MSC-like cells in scleroderma lesional tissue*

Biopsies from the involved forearm skin of patients with recent onset severe diffuse cutaneous subset SSc and from matched sites in healthy controls (HC)(both n=4) were evaluated for the presence of metakaryotic divisions, using 1mm sections cut parallel to the skin surface. Quantification of the number of metakaryotic nuclei in each section was conducted in ten randomly chosen 20x magnification field views per section per biopsy. In the initial screen no metakaryotic nuclei were detected in any of the healthy control sections. In contrast, up to four metakaryotic nuclei were detected in any one 20x magnification field view of the middle and lower sections of SSc biopsies (Figure 1A). Only one metakaryotic cell was detected in the top section of all the SSc sections examined. Middle and lower SSc biopsy sections contained significantly more metakaryotic nuclei than the control samples ( $p < 0.0001$ ) and slightly more metakaryotic nuclei were detected in the deepest section than the middle section (upper HC 0, SSc  $0.05 \pm 0.05$ , middle HC 0, SSc  $1.225 \pm 0.06$   $p < 0.0001$ , lower HC 0, SSc  $1.45 \pm 0.16$   $p < 0.0001$  (mean  $\pm$  SEM)). A range of metakaryotic nuclear forms were seen in the deep SSc sections, including bell forms, pipe shaped forms, and cup shaped forms, in association with thick collagen fibrils (Figure 1B).

Furthermore, vascular abnormalities were frequently seen in SSc where microvascular cells containing multiple small cyst-like structures were observed, possibly reflecting apoptotic blebs, and consistent with the known microvascular damage seen in this disease(8). Metakaryotic cells were found adjacent to these abnormal microvessels in the deep dermis of SSc tissues (Figure 1C). Summary images from each patient sample are shown in Supplementary data Figure S1.

In a further confirmatory analysis (n=4 diffuse SSc patients) samples from involved forearm skin and clinically uninvolved tissue from the back were compared. As before, frequent metakaryotic

forms were seen in the deeper layer fibrotic tissue in association with collagen fibrils. Even in the clinically uninvolved skin, metakaryotic forms were seen in the deep layer fibrotic tissue, and adjacent to abnormal >30µm microvessels which were frequently observed in both involved and clinically uninvolved skin (Table 1). Smaller healthy-looking microvessels (20-30µm) in association with metakaryotic cells were seen in both involved and clinically uninvolved tissue, possibly indicating *de novo* angiogenesis (Figure 1D).

Characteristics	Affected	Unaffected	Control	Comments
Metakaryotic stem cell fraction in mesenchymal, fibrotic sections of the skin.	$3 \pm 1 \times 10^{-3}$	$3 \pm 1 \times 10^{-3}$	$1 \times 10^{-4}$	The thickness of fibrotic parts is two-three times higher in affected skin biopsies compared to unaffected counterparts.
Metakaryotic stem cell fraction in epithelial sections of the skin.	$2 \pm 1 \times 10^{-5}$	$2 \pm 1 \times 10^{-5}$	$1 \times 10^{-5}$	
Diseased, damaged blood vessels (> 30 um diameter).	Yes	Yes	No	~90% of blood vessels in affected skin, ~70% of blood vessels in unaffected skin look damaged or dying (Fig. 2).
Small (20-30 um diameter) normal blood vessels with visible stem cells.	Yes	Yes	Rare	Possible ' <i>de novo</i> ' angiogenesis, attempt to regenerate dead blood vessels.

**Table 1** Analysis of metakaryotic cell frequency in involved and clinically uninvolved SSc skin biopsy material. Metakaryotic divisions were seen in both lesional forearm and non-lesional clinically uninvolved tissue from the back. Metakaryotic divisions were seen within fibrotic tissue in deeper layers, and adjacent to microvasculature.

Additional cytological abnormalities were also seen in the fibrotic material including many binucleated cells with morphologic features indicating the presence of osteoclasts, as well as calcified material (Figure 1E). Osteoclasts, which are derived from macrophages under the influence of myostatin/RANKL(17), are not known to be present normally in the skin and were not found in any of the healthy control sections examined.

#### *Modelling the interaction between SSc disease microenvironment and MSCs.*

In view of the presence of dividing MSC-like cells in the SSc skin, an attempt was made to model and understand how their activation was being initiated within the disease microenvironment.

Human MSCs, derived from subcutaneous fat of healthy controls (16, 18), were maintained in tissue culture with blister fluid (BF) sampled from the forearm skin lesions of patients with recent onset severe diffuse subset SSc, as well as BF from healthy controls (both n=4) diluted 1:125 in 0.2% DMEM. Our recent analysis has implicated the IL-6 family Th2 cytokine IL-31 as having a role in SSc skin and lung fibrosis. IL-31 is secreted by Th2 cells and the receptor IL-31RA/OSMR expressed by tissue resident cells including MSCs. Furthermore, in our analysis IL-31 is present in the dermal blister fluid, at higher levels than other disease-associated cytokines. Therefore, the addition of recombinant IL-31 was used to study the potential effects of a disease microenvironment cytokine. MSCs or normal human dermal fibroblasts (n=4 replicates) were maintained in tissue culture with SSc or healthy control blister fluid (BF), or with IL-31 (50ng/ml), in order to model the effect of the disease microenvironments on resident tissue cells. After 16 hours the cells were lysed for RNA extraction and analysed by Illumina RNAseq technology to profile the patterns of gene expression induced by the SSc BF.

Hierarchical clustering of samples indicated complete separation of MSCs from healthy dermal fibroblasts, indicating that the two cells types have distinct expression profiles regardless of treatment (Figure 2A). Since MSCs are not lineage committed cells, it is expected that they would have an expression profile reflecting their stem-cell pluripotency, while healthy dermal fibroblasts are an established differentiated cell line which express genes related to their function in the skin. Consistent with this *NT5E*, *Thy1* and *Eng* were expressed under basal conditions by MSCs.

Of the candidate genes studied, the largest change in gene expression in the BF treated MSCs was the induction of 3 genes, *CEMIP*, *IL6* and *ACAN*, highly relevant to SSc pathogenesis, and consistent with induction of an invasive tissue repair phenotype in MSCs, not seen in the treated fibroblasts, where the expression of these genes was low. *ACAN* encodes the proteoglycan aggrecan, previously shown to be strongly elevated in SSc skin fibroblast cultures (19). Also, the expression of *ACTA2*, a myofibroblast-associated gene encoding  $\alpha$ -SMA, was higher in SSc BF treated MSCs, compared to healthy control BF treated MSCs. *CTGF* and *COL1A1* were also more highly expressed in SSc BF treated MSCs (Figure 2B). Taken together, these findings indicate myofibroblast commitment of the cells exposed to SSc microenvironment.

*NT5E* which encodes CD73, is a gene relating to the pluripotency of MSCs. SSc blister fluid treatment led to reduced *NT5E* in MSCs indicating commitment to differentiation. It is possible that under SSc blister fluid conditions, MSCs, even as soon as 16 hours after treatment, begin to lose some MSC characteristics and differentiate. Furthermore, physiologically, MSCs express vascular growth factors as part of their role in endothelial and vascular homeostasis. Expression of *VEGFC* was significantly decreased by SSc blister fluid (Figure 2B). Furthermore, *GAS1*, a cell cycle arrest gene, was suppressed by SSc BF treatment, consistent with induction of a proliferative phenotype. However, notably, there was no difference between the treatments with respect to *TGFβ* or *TGFβR* gene expression by MSCs. While a reduction in *THY1* expression has been shown to be indicative of MSC differentiation, the expression of this gene was not affected by the SSc microenvironment treatment. Likewise, fibronectin *FN1* was not upregulated by any of the treatments.

Unlike the findings with MSCs, dermal fibroblasts were less consistently responsive to the specific BF treatments. While some replicate samples clustered together, others clustered with samples from other treatments and did not share the same expression profile (Figure 2A). *ALCAM*, *COL4A1* and *ENG* were downregulated in fibroblasts, as were *CEMIP*, *IL6* and *ACAN*, unlike the induction of these genes seen in MSCs. However, notably,  $\alpha$ -SMA expression was higher in SSc BF treated fibroblasts than control media treated fibroblasts. IL-31, as an SSc microenvironment cytokine, had more of an effect on dermal fibroblasts than on MSCs and induced elevated expression of *CXCL5*, *ANXA1* and *IL-33* involved in angiogenesis, cell adhesion and inflammation respectively.

IL-31 was present at a high level in the BF trending to higher levels in SSc (HC N=15 samples, range 0-21, median 0, SSc N=28, range 0-1117, median 0 pg/ml, P=NS), (Figure 2C), However, in terms of NGS signature IL-31 generally failed to recapitulate the effects of adding SSc BF to the MSCs (Figure 2A&B).

Based on the above findings, it was concluded that SSc microenvironment exposure consistently induces a myofibroblast-like commitment of MSCs, and that the effects on differentiated fibroblasts were less marked and non-consistent.

### *Ingenuity Pathway Analysis of SSc microenvironment treatments*

In addition, Ingenuity Pathway Analysis (IPA) was used to predict signaling pathways and network effects involved in the MSC activation. IPA pathway analysis illustrated the complexity of gene expression in response to SSc microenvironments and implicated both known SSc-related pathways and novel generated disease associated pathways in the MSC activation. Overall, many pro-fibrotic pathways of relevance to complex fibrotic pathology were predicted by the analysis software (Figure 2D). The most significantly activated pathway in response to SSc blister fluid was the integrin linked kinase pathway (*ILK*) (Z-score of -2.52982 with 21.9% overlap between the predicted genes involved and the observed genes)(Figure 2D). Some of the genes in the *ILK* pathway include *ACTA2* and integrins. The *ILK* gene is involved with  $\beta 1$  and  $\beta 3$  integrin-mediated signal transduction, and is associated with multiple cellular functions including cell migration, proliferation, and adhesion (20). Interestingly, aside from this pathway, integrin signaling was found to be reduced by the IPA, supporting the idea that downstream signaling through *ILK* was the dominant integrin-dependent response.

Furthermore, *IL-8*, *NRF2* and *VEGF* signaling were predicted to be reduced by the IPA results. The *VEGF* pathway decreased in response to SSc blister fluid with 21.4% of the known genes of this pathway found differentially expressed in the RNAseq dataset.

Pathways involved in cell migration were upregulated by SSc blister fluid. Both actin cytoskeleton remodelling and Rho based motility are pathways found to be significantly involved in MSCs treated with SSc blister fluid.  $\alpha$ -SMA was implicated to be involved in both processes. Moreover, MSC differentiation is regulated via *RhoA*, which in turn is increased by SSc blister fluid. *RhoA* has influence on cell shape, signalling and cytoskeletal integrity. Signalling via *ROCK*, *RhoA* determines cell shape drives stem cell commitment.

Supportive of MSC differentiation in SSc microenvironments, the *NANOG* pathway, which is associated with pluripotency of mammalian cells, was significantly deactivated.

### *Ingenuity Pathway Analysis: networks of responsive genes*

Aside from predicting individual pathways involved in the response of MSCs to SSc blister fluid, the software created networks of focus molecules linked together based on biological

connectivity. Two significant networks were identified by the software when comparing expression of media control and SSc blister fluid treated MSCs (Shown as Supplementary data Figure S3). One is a network predicted to be involved in connective tissue and organismal injury, and cell morphology, with a high score of 37, consisting of 33 focus nodes. It is centralised around the growth factor *ERBB2*(Figure S3A). Other factors of relevance to the finding of SSc blister fluid induced cell migration are Rho GTPases, also highlighted in this network. Furthermore, osteogenic differentiation associated genes fit into this network, such as *TWIST2*. The second predicted network was focused around connective tissue growth and development (Figure S3B). This pathway is centered around the *CTGF* gene, and, together with *Col1A1*, it is clear that SSc blister fluid induces MSC expression of genes highly associated with SSc fibrosis and myofibroblast activation. MMPs are also part of this network, supporting an effect on migration and tissue remodeling.

#### *Ingenuity Pathway Analysis: predicted upstream regulators*

IPA has the useful ability of predicting upstream regulators that explain the differential expression observed in the RNAseq data. The software uses Knowledge base database to predict biological processes being activated or deactivated by certain molecules and their effects on downstream molecules. P-values calculated by this analysis identify how well the RNAseq measured genes are regulated by a specific regulator and is calculated using Fisher's Exact Test where significance is  $p < 0.01$ . Using this approach,  $TGF\beta$  was predicted to be an upstream regulator of over 100 of the differentially expressed genes analysed. These include *ACTA2*, *ACAN*, collagen genes, Rho GTPases, *TWIST* genes, *NT5E*, *IL6* and *TGF\beta R*, where  $p = 8.62 \times 10^{-30}$  and  $Z = -0.372$ .

Furthermore, of relevance to the female predominance of SSc, the oestrogen receptor was predicted to be a significant upstream regulator of SSc blister fluid induced pathways. A Z-score of 2.534 indicated significant activation and a p-value of  $2.46 \times 10^{-8}$  showing a high level of overlap between observed and theoretical pathway activation. The oestrogen receptor was also a predicted to be a significant upstream regulator for *ANXA1*, *CTGF*, collagen molecules, *NT5E* and MMPs.  $P = 9.95 \times 10^{-15}$  for this regulation and  $Z = -1.769$ .

### *IPA analysis: biologic significance*

Described in Table 2, are the predicted biological functions which differed between treatment conditions. Functions consistently activated by SSc blister fluid when compared to DMEM control, include differentiation and proliferation of multilineage progenitor cells, fibrosis and wound healing, supporting the notion that SSc blister fluid induces MSCs to differentiate into pro-fibrotic wound healing cells. Furthermore, the functions found to be deactivated by SSc blister fluid included functions regarding the development and growth of vasculature, such as the formation of new blood vessels. Fitting these pathways into biological significance shows that most of the involved functions that differ between the two conditions relate to vasculogenesis and angiogenesis. This is a significant finding and may be relevant to the failure to repair the microvasculature in SSc.

Categories	Diseases or Functions Annotation	p-Value	Z-Score	Molecules
Cell Death and Survival	apoptosis	2.44E-39	-0.103	381
Cellular Assembly and Organization, Cellular Function and Maintenance	organization of cytoplasm	1.49E-27	-0.921	234
Tissue Development	growth of epithelial tissue	3.15E-22	-0.757	119
Cellular Assembly and Organization, Tissue Development	fibrogenesis	1.34E-22	-0.42	77
Organismal Injury and Abnormalities	wound	6.22E-16	-0.204	49
Cellular Movement, Connective Tissue Development and Function	cell movement of fibroblast cell lines	1.69E-15	-0.495	48
Cellular Assembly and Organization, Cellular Function and Maintenance, Tissue Development	formation of actin stress fibres	7.15E-15	-1.193	50
Cardiovascular System Development and Function, Cellular Movement	migration of vascular endothelial cells	2.42E-14	-1.335	39
Cellular Development, Connective Tissue Development	differentiation of osteoblasts	3.51E-14	0.217	53
Connective Tissue Development and Function, Tissue Morphology	quantity of connective tissue cells	1.23E-11	-1.309	48
Cellular Movement	cellular infiltration	2.65E-10	-1.103	68
Cell-To-Cell Signalling and Interaction, Cellular Assembly and Organization, Cellular Function and Maintenance	formation of focal adhesions	1.24E-13	-1.53	35
Organismal Development	growth of vessel	1.81E-11	1.871	32
Cellular Development, Connective Tissue Development	differentiation of adipocytes	1.59E-09	0.069	43

Cellular Development, Connective Tissue Development	differentiation of chondrocytes	4.23E-09	0.719	24
Cardiovascular System Development and Function	vascularization	5.99E-12	0.383	46

**Table 2** Ingenuity pathway analysis (IPA) indicated that SSc BF when compared to DMEM media alone, had induced multiple pathways (no shading) including apoptosis of cells, epithelial growth, fibrogenesis, wound repair, cell movement, osteoblast differentiation and infiltration, as well as down regulation (shaded grey) of vasculogenesis, adipogenesis, and chondrogenesis, when compared to controls treated with media only.

Although the healthy control BF induced some of the changes seen with SSc BF, but lesser in magnitude (Figure 2A&B), significant differences were demonstrated between the two treatments (Table 3). Compared to healthy control BF, SSc BF induced cell differentiation, proliferation of multilineage progenitor cells, wound healing, fibrosis and necrosis, whereas endothelial cell proliferation, vessel formation, angiogenesis and vasculogenesis were decreased (Table 3).

Categories	Diseases or Functions Annotation	p-Value	Z-Score	Molecules
Cellular Development	differentiation of cells	5.89E-13	3.169	81
Cellular Growth and Proliferation, Organismal Development	proliferation of multilineage progenitor cells	1.28E-07	0.838	9
Organismal Injury and Abnormalities, Tissue Morphology	healing of wound	2.22E-07	1.254	13
Organismal Injury and Abnormalities	fibrosis	1.03E-08	0.092	29
Cell Death and Survival	necrosis	5.62E-14	0.57	93
Cellular Growth and Proliferation	cell proliferation of vascular endothelial cells	6.47E-07	-0.633	11
Embryonic Development, Organismal Development	development of body axis	7.16E-07	-0.373	40
Organismal Development	formation of vessel	7.25E-07	-0.786	11
Cell-To-Cell Signalling and Interaction, Hematological System	activation of blood cells	7.27E-07	-2.047	27
Hematological System Development and Function, Tissue Morphology	quantity of blood cells	7.54E-07	-1.756	39
Cardiovascular System Development and Function, Organismal Development	angiogenesis	1.53E-16	-2.465	52

Cardiovascular System Development and Function, Organismal Development	vasculogenesis	1.88E-15	-2.615	45
Cardiovascular System Development and Function	development of vasculature	1.83E-14	-2.464	53

**Table 3** Comparison was made between SSc BF treated and control BF treated MSCs, revealing pathways induced by SSc (no shading) or decreased by SSc vs control (shaded grey). Significantly altered pathways induced by SSc included proliferation of progenitor cells, wound healing, fibrosis and necrosis, whereas pathways relating to endothelial cell proliferation, body axis development and angiogenesis were inhibited by the SSc BF treatment.

Comparison was made with the results of Gene Ontology biologic process analysis, which in general confirmed enhanced fibrogenesis, collagen synthesis, connective tissue repair, as well as dysregulated angiogenesis and vascular repair (Supplementary data Tables S1 and S2). Overlap with the IPA included differentiation of osteoblasts, formation of focal adhesions, actin filament formation (enhanced by SSc BF), as well as cardiovascular development and morphogenesis (reduced).

#### *Phenotypic changes induced in MSCs by scleroderma blister fluid*

Because of the above findings we went on to attempt to validate phenotype changes implicated in the NGS, by modelling using MSCs maintained in tissue culture. The induction of  $\alpha$ SMA, indicating myofibroblast differentiation pattern, was investigated further by qPCR. A significant difference between  $\alpha$ SMA expression induced by SSc blister fluid compared with healthy control blister fluid was observed even when diluted 1:125 in DMEM (HC blister fluid treated  $3.9 \pm 0.5$ , SSc blister fluid treated MSCs  $8.4 \pm 1.6$ ,  $p=0.048$  mean  $\pm$  SEM, expression relative to basal) (Figure 3A). Furthermore, since TGF $\beta$  had been implicated as an extracellular driver of the NGS changes, its potential role was investigated further. SSc blister fluid diluted 1:125 induced  $\alpha$ SMA expression equivalent to addition of TGF $\beta$  (4ng/ml) (media control  $16.8 \pm 1.2$ , SSc blister fluid treated  $29.4 \pm 1.1$ ,  $p<0.0004$ , TGF $\beta$  treated  $32.7 \pm 1.8$ ,  $p<0.004$ , relative expression), and the stimulatory effect of SSc BF was antagonised by the TGF $\beta$ 1-3 inhibitory antibody 1D11 (mean  $10.3 \pm 0.4$ ,  $p<0.0001$ ) supporting a central role for TGF $\beta$  in the SSc BF effects (Figure 3B). Also, further BF samples taken from healthy controls and SSc patients were assayed to confirm the presence of TGF $\beta$ , which trended to higher levels in the patient samples (TGF $\beta$  HC range 78-667,

mean 288, SSc 136-696, mean 328pg/ml P=NS) ( Figure 3C). In addition, inhibitors of PI3K signalling (Wortmannin), and the ERK inhibitor (U0126) blocked the  $\alpha$ SMA induction by SSc BF, implicating these signalling pathways ( $p < 0.0001$  for each inhibitor vs SSc BF treated). Based on these experiments it was concluded that in monolayer culture, induction of  $\alpha$ SMA in MSCs by SSc blister fluid is dependent on TGF $\beta$  plus signalling via PI3K and ERK.

Scratch wound migration was used as a measure of invasiveness/spreading of activated MSCs in the SSc microenvironment (Figure 3D). Compared to medium control, SSc BF induced MSC scratch migration (residual scratch area at 24 hours, control  $1.33 \pm 0.09$ , SSc BF treated  $0.72 \pm 0.11$  mean  $\pm$  SEM mm<sup>2</sup>,  $p < 0.016$ ) equivalent to 10% serum positive control. IL-31 appeared to enhance migration of MSCs (but P NS), inhibited by Wortmanin implicating PI3K.

Furthermore, the SSc BF induced collagen gel contraction by the MSCs, consistent with a differentiation into contractile myofibroblast-like cells (residual gel mass in media control  $0.11 \pm 0.008$  g, SSc blister fluid treated  $0.066 \pm 0.009$ , mean  $\pm$  SEM g,  $p = 0.002$ ) (Figure 3E).

Since loss of adipose tissue is associated with severe skin involvement in SSc, the effects of SSc BF were explored in an MSC adipogenesis assay, indicating partial inhibition of the adipogenic commitment by the SSc BF (trending but P NS) and consistent with the pathway analysis (Figure 3F).

Furthermore, protein assays for  $\alpha$ SMA, collagen I and the matricellular protein CTGF (each N=3 replicates) were used to validate the myofibroblast-like transdifferentiation of MSCs. SSc BF induced these protein factors, more than control BF and consistent with some kind of pro-fibrotic transdifferentiation of the MSCs. The changes were fully antagonised by addition of SB431542 (10uM), a small molecule inhibitor of Alk4,5&7(21) (Figure 3G&H).

#### *Role of mechanosensing in SSc microenvironment*

Since the ILK and RhoA pathways had been implicated in the IPA analysis, and because increased stiffness (mechanical stress) in affected tissues is a hallmark feature of SSc (22), it was hypothesised that mechanosensing might be an important factor in determining the activation of MSCs within the disease microenvironment. We measured the effect of altered substrate ECM and also tested the effect of adding the mechanosensing inhibitor of MRTF-A signalling CCG-

1423(23) on the induction of MSCs. 4kPa and 50kPa Softwell gel culture matrices were used to model soft healthy control skin and stiff scleroderma skin matrices respectively in N=4 replicate experiments.  $\alpha$ SMA could not be effectively induced on the soft matrices by either SSc BF treatment or by TGF $\beta$ , but could be fully induced on 50kPa gels (on 50kPa gels, control  $1.85\pm 0.49$ , TGF $\beta$  treated  $99.5\pm 41$ ,  $p < 0.007$ , on 4kPa control  $2.55\pm 1.8$ , TGF $\beta$  treated  $1.93\pm 1.7$ , pNS relative expression) (Figure 4A&B). By contrast, CTGF, an early response matricellular protein, could be induced on both soft and stiff gels (on 50kPa control  $19.8\pm 6.03$ , TGF $\beta$  treated  $598\pm 85.1$ ,  $p < 0.029$ , on 4kPa control  $18.3\pm 6.96$ , TGF $\beta$  treated  $465\pm 349$ , pNS, relative expression). Both  $\alpha$ SMA and CTGF were suppressed fully by CCG-1423 ( $\alpha$ SMA in TGF $\beta$ +CCG-1423 treated,  $0.59\pm 0.20$   $p < 0.0061$ , CTGF in TGF $\beta$ +CCG-1423 treated,  $1.67\pm 1.09$   $p < 0.045$ ) consistent with dependence on MRTF-A signaling and mechanosensing (Figure 4A&B).

Also, since ectopic bone formation (calcinosis) is a significant problem for SSc patients, occurring at sites of pressure or enhanced mechanical stress, an attempt was made to model the osteogenic differentiation of MSCs on soft or stiff gels. Osteogenic differentiation could not be effectively induced on the soft 4 kPa gels, but was induced by both TGF $\beta$  and IL-31 on 50kPa gels (on 4kPa gels, control  $0.33\pm 0.33$ , TGF $\beta$  treated  $0.667\pm 0.33$ , IL-31 treated  $0\pm 0$ ), CCG-1423 treated  $0\pm 0$ , on 50kPa gels control  $1.67\pm 0.33$ , TGF $\beta$  treated  $3\pm 0$ , IL-31 treated  $3.33\pm 0.33$ , CCG-1423 treated  $0.33\pm 0.33$ , Aluzarin red assay (0-4))(Figure 4C).

It was concluded that mechanical stress in the disease microenvironment is likely a determinant of the potential activation of MSCs, including their commitment to myofibroblast or else osteoblast dependent on the context, and that growth factors and cytokines were capable of inducing osteogenic differentiation in these cells, dependent on a stiff extracellular matrix.

#### *Effect of lactate in blister fluid on MSC myofibroblast commitment*

Furthermore, since there is failure of angiogenesis, plus the presence of microvascular damage and ischaemia in SSc, lactate as a product of glycolytic metabolism is a potential factor acting within the SSc disease microenvironment. Lactate is transported into and out of mitochondria via a lactate-protein co-transporter which is inhibited by  $\alpha$ -cyano-4-hydroxycinnamic acid ( $\alpha$ CHCA)(24). Accordingly, MSCs in monolayer culture were treated with SSc or control BF with

or without  $\alpha$ CHCA and then assayed by qPCR for  $\alpha$ SMA. These experiments indicated that as expected SSc BF induced  $\alpha$ SMA, but dependent on the presence of lactate (Figure S2A). The lactate inhibitor suppressed  $\alpha$ SMA levels to near zero and below basal levels supporting the idea that presence of lactate is a required factor for myofibroblast commitment (control  $\alpha$ SMA  $43.9\pm 5.9$ , SSc BF treated  $57.3\pm 4.4$ , SSc BF+  $\alpha$ CHCA treated  $15.5\pm 4.6$   $p<0.015$ ).

SSc and control BF samples were assayed for the presence of lactate, showing lactate present in the 10-60mM range and trending to higher levels in the disease (control BF range 8-36, mean 24 SSc BF range 14-62, mean 48mmol/l,  $P=NS$ ) (Figure S2B). Furthermore, as shown in Figure S2C, SSc BF, but not control BF, induced gel contraction similar to positive control with 10% serum (DMEM control  $0.13\pm 0.026$ , SSc blister fluid  $0.08\pm 0.007$ , healthy control blister fluid  $0.16\pm 0.002$ , residual gel mass at 24hrs in g,  $p=0.023$ ). Lactate treatment of MSCs failed to significantly alter gel contraction (lactate treated  $0.108\pm 0.019$  g,  $p=NS$ ). Furthermore, addition of the lactate inhibitor did not significantly alter SSc BF induced gel contraction (Figure S2C). It was concluded that lactate transport into mitochondria is a required factor for  $\alpha$ SMA induction, but not required for SSc BF induced contractility in MSCs.

## Discussion

This is the first study to demonstrate the presence of metakaryotic cell divisions, believed to represent dividing MSCs, in SSc skin, in association with thick collagen fibrils in the deeper layers of the dermis and adjacent to damaged microvessels in both involved and clinically unaffected skin. Such metakaryotic divisions were recently described as being characteristic of dividing tissue resident stem cells, seen during organogenesis and then recapitulated during wound healing or in pathologic tissue remodeling, such as cancer or atherosclerosis (14). The findings support the idea that MSCs are being activated and dividing in the SSc tissues at an early stage of disease development, and are consistent with current concepts regarding the role of these cells in fibrosis (7, 25). In general, previous work has demonstrated that the deeper dermis is the predominant site of  $\alpha$ SMA expressing cells, where myofibroblast activation appears maximal in this disease.

Furthermore, our findings support the idea that adipose derived MSCs are becoming activated through exposure to the early disease microenvironment, differentiating towards damaging profibrotic cells, and away from potentially beneficial reparative effects such as vascular repair, cartilage repair and maintenance of subcutaneous fat. These findings confirm previous studies indicating that MSCs can commit to become tissue resident myofibroblast-like cells, demonstrated by lineage tracing in multiple mouse models of fibrotic disease (26-32). Most notably, Varga and colleagues have demonstrated in the bleomycin mouse model, that subcutaneous fat derived stem cells transdifferentiate to myofibroblasts present in the deep dermal layer of the fibrotic lesions (32). Furthermore, previous studies have demonstrated MSC-like cells (pericytes) as migrating from perivascular sites in SSc tissue and showing intermediary stage cells consistent with myofibroblast trans-differentiation (33). Moreover, gene expression profiling indicates that MSCs exposed to the SSc microenvironment undergo multiple phenotype changes consistent with migration/invasion, wound healing, connective tissue development and enhanced osteogenic commitment, as well as loss of adipogenesis. These changes could account for the chronic and excessive tissue repair seen as well as the loss of subcutaneous adipose cells seen both in SSc and wounds (32).

However, counter to the proposal that MSCs have a damaging profibrotic role in SSc, are previous findings that these cells may have restorative anti-inflammatory and immunosuppressive effects likely to be of benefit in autoimmune disorders. For example, umbilical cord derived MSCs have been shown to attenuate inflammation and fibrosis in a mouse model of SSc lung fibrosis (34). It may be that any beneficial therapeutic effects would best be utilized in the late stage disease, such as in autologous fat transplantation used as a regenerative therapy in late atrophic phase SSc (35).

Pathway analysis predicted that TGF $\beta$  as well as estrogen receptor agonists were important upstream inducers of the changes seen in MSCs exposed to SSc microenvironment, consistent with current models of fibrosis indicating an essential role for TGF $\beta$  and also supporting a role for estradiol in driving SSc fibrosis (36, 37). Inhibition of TGF $\beta$  abolished the myofibroblast transdifferentiation of MSCs indicating that it might be driving the MSC commitment. However,

mechanosensing and the presence of lactate were also demonstrated as being required factors present in the microenvironment.

The osteogenic commitment seen is also highly relevant to the calcinosis seen in SSc, which is a severely disabling manifestation of the disease(9). In general, such ectopic bone tissue formation is seen at sites of trauma and mechanical stress and as shown here depends on mechanosensing (38). IL-31, an IL-6 family member cytokine, present at high levels in the tissue fluid, might contribute to the enhanced migration and osteogenic differentiation, but only partially accounted for the full spectrum of changes seen in MSC activation.

Although the exact cellular origin of myofibroblasts in dermal fibrotic lesions is not exactly known, it is likely that there are multiple contributing sources such as tissue resident fibroblasts, circulating monocyte like cells (fibrocytes)(39), as well as cells transitioning through an EMT-like process(40), or through EndoMT(41), as well as perivascular stem cells (33). Our study indicates that subcutaneous adipose MSCs are a further potential source of the pathogenic myofibroblasts. In mice lineage tracing experiments have indicated that a specific subset of MSCs (Lck+ Sca-) are responsible for maintaining the deep dermal and subdermal tissues and that these cells are responsible for the overproduction of extracellular matrix in the early stages of wound healing (42). It is possible that the human equivalent cells are involved in driving SSc pathogenesis, accounting for the fibrosis which is predominantly affecting the deep dermis, and is associated with loss of subcutaneous adipose tissues.

There are certain limitations of this study, including the relatively small number of skin and tissue fluid samples analysed, and the use of healthy donor adipose MSCs rather than lesional MSCs in the tissue culture experiments. However, taken together, the overall picture that emerges is of multiple factors in the disease microenvironment inducing adipose MSC commitment to pathogenic myofibroblasts. These effects on MSCs seem to be more specific than the effects on differentiated dermal fibroblasts. Several inhibitory treatments were assessed, including anti-TGF $\beta$  antagonists, as well as pathway signaling inhibitors, and lactate response antagonists, each of which suppressed the MSC to myofibroblast differentiation. Such antagonists, if they could safely be used, could arrest the development of this and other fibrotic diseases.

## References

1. Allanore Y, Simms R, Distler O, Trojanowska M, Pope J, Denton CP, et al. Systemic sclerosis. *Nature reviews Disease primers*. 2015;1:15002.
2. Varga JA, Trojanowska M. Fibrosis in systemic sclerosis. *Rheum Dis Clin North Am*. 2008;34(1):115-43; vii.
3. Clark KE, Lopez H, Abdi BA, Guerra SG, Shiwen X, Khan K, et al. Multiplex cytokine analysis of dermal interstitial blister fluid defines local disease mechanisms in systemic sclerosis. *Arthritis research & therapy*. 2015;17:73.
4. da Silva Meirelles L, Chagastelles PC, Nardi NB. Mesenchymal stem cells reside in virtually all post-natal organs and tissues. *Journal of cell science*. 2006;119(Pt 11):2204-13.
5. Bianco P, Cao X, Frenette PS, Mao JJ, Robey PG, Simmons PJ, et al. The meaning, the sense and the significance: translating the science of mesenchymal stem cells into medicine. *Nature medicine*. 2013;19(1):35-42.
6. Crisan M, Yap S, Casteilla L, Chen CW, Corselli M, Park TS, et al. A perivascular origin for mesenchymal stem cells in multiple human organs. *Cell stem cell*. 2008;3(3):301-13.
7. El Agha E, Kramann R, Schneider RK, Li X, Seeger W, Humphreys BD, et al. Mesenchymal Stem Cells in Fibrotic Disease. *Cell stem cell*. 2017;21(2):166-77.
8. Altorok N, Wang Y, Kahaleh B. Endothelial dysfunction in systemic sclerosis. *Current opinion in rheumatology*. 2014;26(6):615-20.
9. Valenzuela A, Chung L. Calcinosis: pathophysiology and management. *Current opinion in rheumatology*. 2015;27(6):542-8.
10. Wei J, Melichian D, Komura K, Hinchcliff M, Lam AP, Lafyatis R, et al. Canonical Wnt signaling induces skin fibrosis and subcutaneous lipoatrophy: a novel mouse model for scleroderma? *Arthritis and rheumatism*. 2011;63(6):1707-17.
11. Thilly WG, Gostjeva EV, Koledova VV, Zukerberg LR, Chung D, Fomina JN, et al. Metakaryotic stem cell nuclei use pangenomic dsRNA/DNA intermediates in genome replication and segregation. *Organogenesis*. 2014;10(1):44-52.
12. van den Hoogen F, Khanna D, Fransen J, Johnson SR, Baron M, Tyndall A, et al. 2013 classification criteria for systemic sclerosis: an American College of Rheumatology/European League against Rheumatism collaborative initiative. *Arthritis and rheumatism*. 2013;65(11):2737-47.
13. Sondergaard K, Stengaard-Pedersen K, Zachariae H, Heickendorff L, Deleuran M, Deleuran B. Soluble intercellular adhesion molecule-1 (sICAM-1) and soluble interleukin-2 receptors (sIL-2R) in scleroderma skin. *Br J Rheumatol*. 1998;37(3):304-10.
14. Gostjeva EV, Zukerberg L, Chung D, Thilly WG. Bell-shaped nuclei dividing by symmetrical and asymmetrical nuclear fission have qualities of stem cells in human colonic embryogenesis and carcinogenesis. *Cancer genetics and cytogenetics*. 2006;164(1):16-24.
15. Chieco P, Derenzini M. The Feulgen reaction 75 years on. *Histochemistry and cell biology*. 1999;111(5):345-58.
16. Jin HJ, Bae YK, Kim M, Kwon SJ, Jeon HB, Choi SJ, et al. Comparative analysis of human mesenchymal stem cells from bone marrow, adipose tissue, and umbilical cord blood as sources of cell therapy. *International journal of molecular sciences*. 2013;14(9):17986-8001.

17. Dankbar B, Fennen M, Brunert D, Hayer S, Frank S, Wehmeyer C, et al. Myostatin is a direct regulator of osteoclast differentiation and its inhibition reduces inflammatory joint destruction in mice. *Nature medicine*. 2015;21(9):1085-90.
18. Abignano G, Buch M, Emery P, Del Galdo F. Biomarkers in the management of scleroderma: an update. *Curr Rheumatol Rep*. 2011;13(1):4-12.
19. Westergren-Thorsson G, Coster L, Akesson A, Wollheim FA. Altered dermatan sulfate proteoglycan synthesis in fibroblast cultures established from skin of patients with systemic sclerosis. *The Journal of rheumatology*. 1996;23(8):1398-406.
20. Hannigan GE, Leung-Hagesteijn C, Fitz-Gibbon L, Coppolino MG, Radeva G, Filmus J, et al. Regulation of cell adhesion and anchorage-dependent growth by a new  $\beta$ 1-integrin-linked protein kinase. *Nature*. 1996;379:91.
21. Laping NJ, Grygielko E, Mathur A, Butter S, Bomberger J, Tweed C, et al. Inhibition of transforming growth factor (TGF)- $\beta$ 1-induced extracellular matrix with a novel inhibitor of the TGF- $\beta$  type I receptor kinase activity: SB-431542. *Mol Pharmacol*. 2002;62(1):58-64.
22. Shiwen X, Stratton R, Nikitorowicz-Buniak J, Ahmed-Abdi B, Ponticos M, Denton C, et al. A Role of Myocardin Related Transcription Factor-A (MRTF-A) in Scleroderma Related Fibrosis. *PLoS One*. 2015;10(5):e0126015.
23. Evelyn CR, Wade SM, Wang Q, Wu M, Iniguez-Lluhi JA, Merajver SD, et al. CCG-1423: a small-molecule inhibitor of RhoA transcriptional signaling. *Molecular cancer therapeutics*. 2007;6(8):2249-60.
24. Halestrap AP, Denton RM. Specific inhibition of pyruvate transport in rat liver mitochondria and human erythrocytes by alpha-cyano-4-hydroxycinnamate. *The Biochemical journal*. 1974;138(2):313-6.
25. Lemos DR, Duffield JS. Tissue-resident mesenchymal stromal cells: Implications for tissue-specific antifibrotic therapies. *Science translational medicine*. 2018;10(426).
26. Jun D, Garat C, West J, Thorn N, Chow K, Cleaver T, et al. The pathology of bleomycin-induced fibrosis is associated with loss of resident lung mesenchymal stem cells that regulate effector T-cell proliferation. *Stem cells (Dayton, Ohio)*. 2011;29(4):725-35.
27. Humphreys BD, Lin SL, Kobayashi A, Hudson TE, Nowlin BT, Bonventre JV, et al. Fate tracing reveals the pericyte and not epithelial origin of myofibroblasts in kidney fibrosis. *The American journal of pathology*. 2010;176(1):85-97.
28. Kramann R, Schneider RK, DiRocco DP, Machado F, Fleig S, Bondzie PA, et al. Perivascular Gli1+ progenitors are key contributors to injury-induced organ fibrosis. *Cell stem cell*. 2015;16(1):51-66.
29. Xie T, Liang J, Liu N, Huan C, Zhang Y, Liu W, et al. Transcription factor TBX4 regulates myofibroblast accumulation and lung fibrosis. *The Journal of clinical investigation*. 2016;126(8):3063-79.
30. Marriott S, Baskir RS, Gaskill C, Menon S, Carrier EJ, Williams J, et al. ABCG2pos lung mesenchymal stem cells are a novel pericyte subpopulation that contributes to fibrotic remodeling. *American journal of physiology Cell physiology*. 2014;307(8):C684-98.
31. Carlson S, Trial J, Soeller C, Entman ML. Cardiac mesenchymal stem cells contribute to scar formation after myocardial infarction. *Cardiovascular research*. 2011;91(1):99-107.

32. Marangoni RG, Korman BD, Wei J, Wood TA, Graham LV, Whitfield ML, et al. Myofibroblasts in murine cutaneous fibrosis originate from adiponectin-positive intradermal progenitors. *Arthritis & rheumatology (Hoboken, NJ)*. 2015;67(4):1062-73.
33. Rajkumar VS, Sundberg C, Abraham DJ, Rubin K, Black CM. Activation of microvascular pericytes in autoimmune Raynaud's phenomenon and systemic sclerosis. *Arthritis and rheumatism*. 1999;42(5):930-41.
34. Moroncini G, Paolini C, Orlando F, Capelli C, Grieco A, Tonnini C, et al. Mesenchymal stromal cells from human umbilical cord prevent the development of lung fibrosis in immunocompetent mice. *PLoS One*. 2018;13(6):e0196048.
35. Griffin MF, Almadori A, Butler PE. Use of Lipotransfer in Scleroderma. *Aesthet Surg J*. 2017;37(suppl\_3):S33-S7.
36. Soldano S, Montagna P, Brizzolara R, Sulli A, Parodi A, Seriola B, et al. Effects of estrogens on extracellular matrix synthesis in cultures of human normal and scleroderma skin fibroblasts. *Ann N Y Acad Sci*. 2010;1193:25-9.
37. Rice LM, Padilla CM, McLaughlin SR, Mathes A, Ziemek J, Goummih S, et al. Fresolimumab treatment decreases biomarkers and improves clinical symptoms in systemic sclerosis patients. *The Journal of clinical investigation*. 2015;125(7):2795-807.
38. Yu-Wai-Man C, Spencer-Dene B, Lee RMH, Hutchings K, Lisabeth EM, Treisman R, et al. Local delivery of novel MRTF/SRF inhibitors prevents scar tissue formation in a preclinical model of fibrosis. *Scientific reports*. 2017;7(1):518.
39. Grieb G, Bucala R. Fibrocytes in Fibrotic Diseases and Wound Healing. *Advances in wound care*. 2012;1(1):36-40.
40. Nikitorowicz-Buniak J, Denton CP, Abraham D, Stratton R. Partially Evoked Epithelial-Mesenchymal Transition (EMT) Is Associated with Increased TGFbeta Signaling within Lesional Scleroderma Skin. *PLoS One*. 2015;10(7):e0134092.
41. Manetti M, Romano E, Rosa I, Guiducci S, Bellando-Randone S, De Paulis A, et al. Endothelial-to-mesenchymal transition contributes to endothelial dysfunction and dermal fibrosis in systemic sclerosis. *Annals of the rheumatic diseases*. 2017;76(5):924-34.
42. Driskell RR, Lichtenberger BM, Hoste E, Kretzschmar K, Simons BD, Charalambous M, et al. Distinct fibroblast lineages determine dermal architecture in skin development and repair. *Nature*. 2013;504(7479):277-81.

## Figures

**Figure 1 Metakaryotic stem cells in affected, unaffected SSc and normal skin biopsies.** (A) Skin biopsies from the involved forearm skin of diffuse cutaneous SSc patients, and of matched sites in healthy controls, were assessed for the presence of metakaryotic cells applying  $\sim 1 \times 1$  mm thick biopsy tissue parts (in 'A') spreading and Feulgen's stain to visualize bell shaped nuclei (red arrows) characteristic of metakaryotic cells. Histopathological slides of each section were scanned at x20 objective light microscopy to localize and count metakaryotic cells. Metakaryotic nuclei in fibrotic part of skin biopsy of healthy control were detected at very low frequency  $\sim 1 \times 10^{-5}$ . In 'upper' section of biopsies, mostly presented by epithelial tissues and little of collagen deposition, the frequency of metakaryotic cells was higher in affected SSc biopsies,  $\sim 1 \times 10^{-3}$ . In contrast, the middle and lower sections of SSc biopsies characterized by extensive thickness of collagen fibrils, the fraction of metakaryotic cells reaches  $\sim 3 \pm 1 \times 10^{-3}$ . (B) Examples of metakaryotic cells (bell shaped nuclei, arrowed) amitotic divisions (symmetrical, left panel; asymmetrical, right panel) as seen in fibrotic parts of SSc with extensive deposition of collagen. (C) Abnormal blood vessels with multiple bleb like structures consistent with endothelial cell apoptosis.  $\sim 90\%$  of 10-20  $\mu\text{m}$  and 30-60  $\mu\text{m}$  diameter blood vessels were abnormal /dying in affected SSc and  $\sim 50\text{-}70\%$  in unaffected skin biopsies. No abnormal blood vessels were observed in healthy controls. (D) Normal looking small ( $\sim 10 \mu\text{m}$ ) blood vessels in affected and unaffected SSc skin with 'attached' metakaryotic stem cells (arrowed) are probably 'de novo' angiogenesis, blood vessels regeneration. (E) Furthermore, osteoclasts (arrows) were seen in parts with 'damaged' blood vessels (left panel) as well as in thick collagenous parts (right panel) only in affected SSc sections in addition to microscopic calcinotic material.

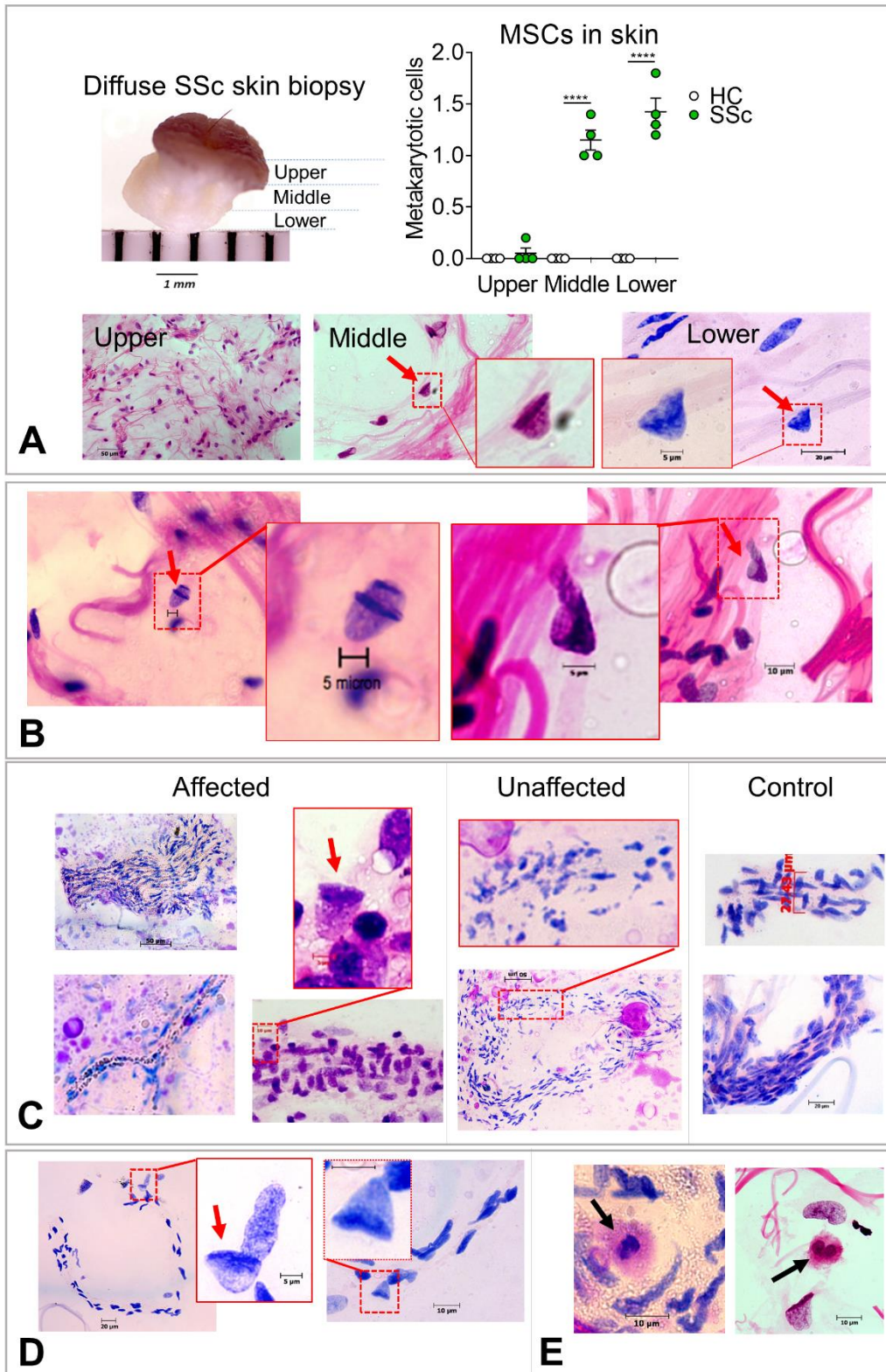


**Figure 2 Effect of scleroderma disease lesional blister fluid and microenvironment cytokine IL-31 on gene expression by MSCs.** (A) SSc blister fluid or control BF each diluted 1:125 in DMEM or recombinant IL-31 (50ng/ml) were added to MSCs in standard tissue culture media and gene expression profiled by Illumina NGS after 16 hours. Hierarchical clustering indicated clear separation of the 2 cell types; 1-16 representing MSC samples and 33-48 healthy dermal fibroblast. Distinct patterns of gene expression leading to hierarchical clustering of candidate factors were consistently induced in MSCs but not fibroblasts by SSc BF. (B) Significantly increased gene expression was seen in factors relevant to myofibroblast differentiation, *ACTA2*, *COL1* and *CTGF*. Furthermore, there was loss of stem cell marker *NT5E* and growth arrest gene *GAS1*. Changes in gene expression were generally greater in magnitude with SSc BF versus control BF, and in general not recapitulated by IL-31 (50 ng/ml) treatment, although as shown in (C) high levels of IL-31 were present in the BF. (D) IPA predicted activation of signalling pathways including *ILK*, *Rho* and *IL6*.

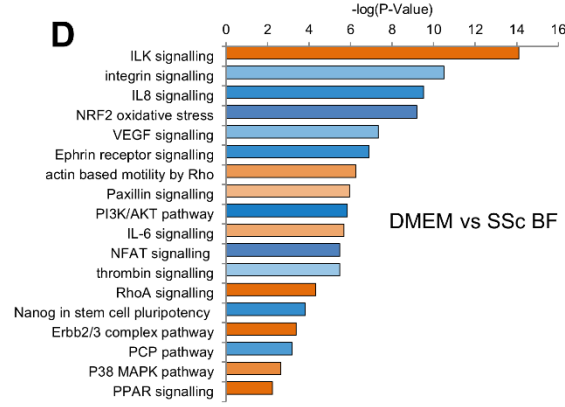
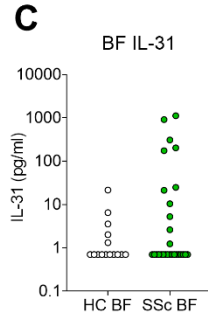
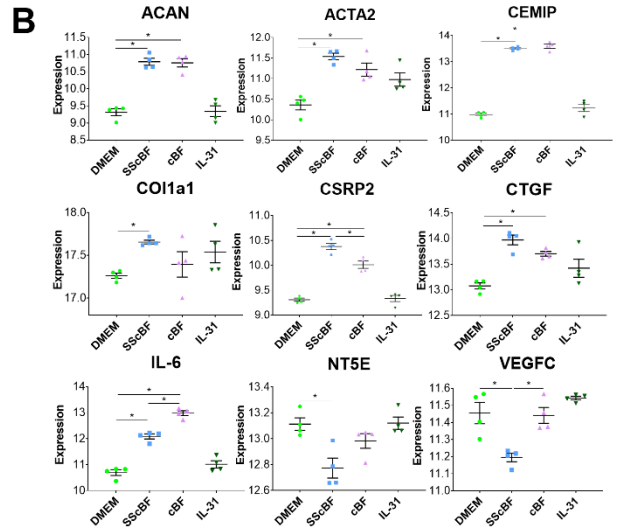
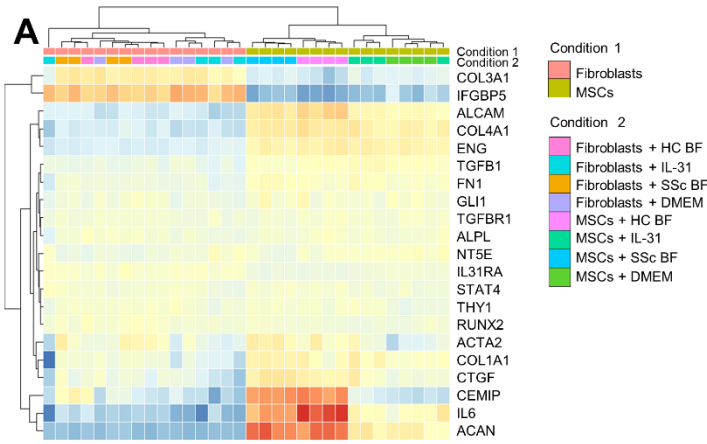


**Figure 3 Phenotypic changes induced in MSCs by scleroderma blister fluid: role of TGF $\beta$**  (A) qPCR

analysis of MSCs indicated that SSc BF, even when diluted 1:125 induced  $\alpha$ SMA, more than control samples, consistent with myofibroblast commitment. (B) MSCs were treated with serum free media, TGF $\beta$  (4 ng/ml), SSc and healthy control blister fluid (BF) (1:125) with or without 1D11 (10  $\mu$ g/ml), Wortmannin (100 nM) and/or U0126 (5  $\mu$ M). SSc blister fluid significantly induced more  $\alpha$ -SMA expression compared to serum free media ( $p=0.0004$ ) and healthy control blister fluid ( $p=0.048$ ), an effect which was fully inhibited by the TGF $\beta$  antibody 1D11. Signalling pathway inhibitors Wortmannin and U0126, also fully reversed SSc blister fluid (both  $p<0.0001$ ). (C) Levels of TGF $\beta$ 1 in SSc and control BF. (D) Scratch wound assays SSc BF and the cytokine IL-31 induced migration equivalent to 10% serum positive control. By 24 hours 10% positive control had induced migration  $p=0.03$  vs 0.2% serum. Also SSc BF induced migration more than 0.2% serum controls,  $p=0.016$ . Furthermore, the addition of Wortmannin inhibited migration induced by IL-31,  $p=0.027$  IL31 vs IL31+W. (E) MSC populated gel contraction at 24 hours indicated that SSc BF enhanced contractility measured by loss of gel weight (g) ( $p=0.002$ ), similar to 10% serum as positive control ( $p=0.0062$ ). IL-31 and control blister fluid (cBF) by comparison, did not result in significant gel weight loss. (F) Oil red O assay at 10 days confirmed suppression of adipogenesis by SSc blister fluid (but P NS). (G,H) Western blotting was used to demonstrate myofibroblast-like commitment of MSCs following treatment with SSc BF more than control BF and antagonised by the TGF $\beta$  signalling inhibitor SB431542. N=3 replicates for each experiments.  $*$ = $p<0.05$ ,  $**$ = $p<0.01$ ,  $***$ = $p<0.001$ ,  $****$ = $p<0.0001$  determined by one-way ANOVA with Tukey's Post Hoc test for multiple comparisons. AM=adipogenic media, HC=healthy control, SSc=scleroderma BF=blister fluid.

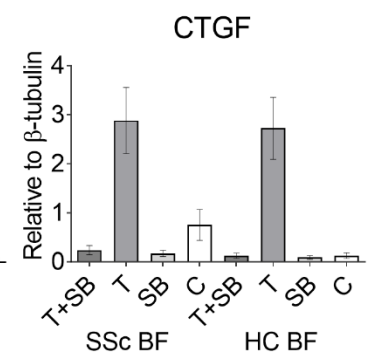
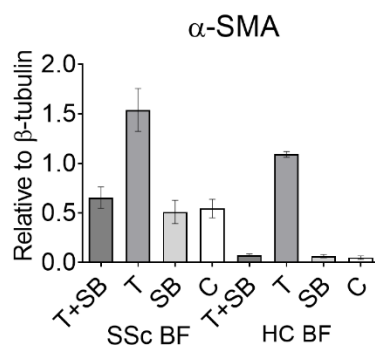
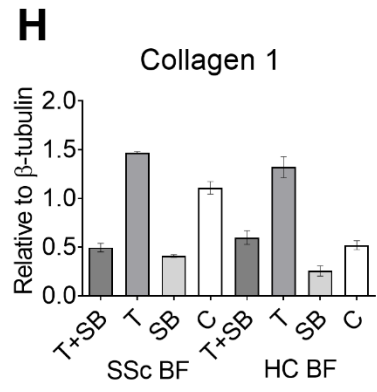
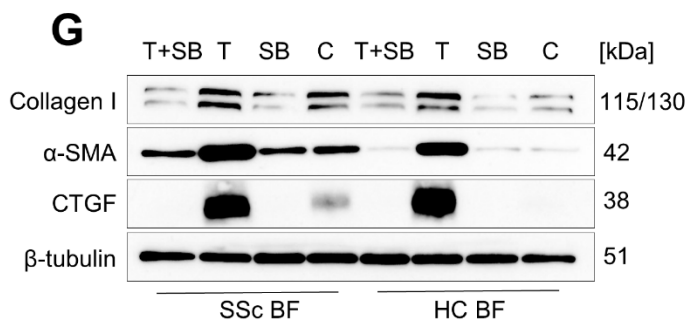
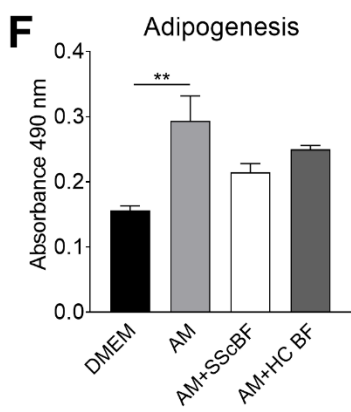
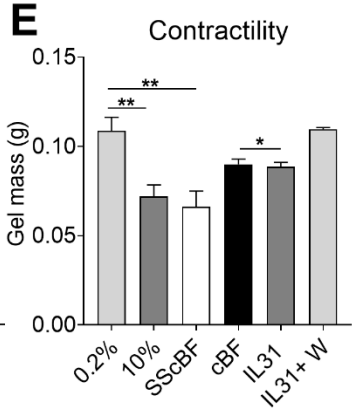
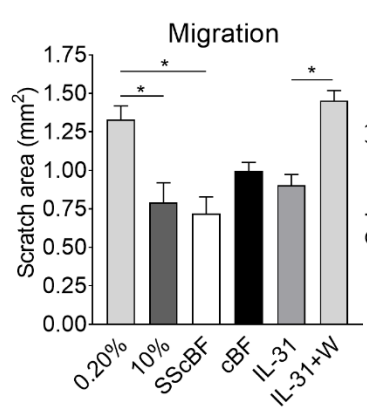
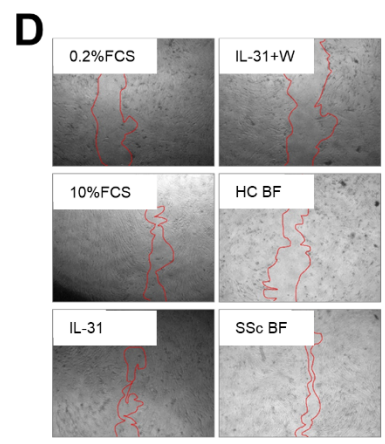
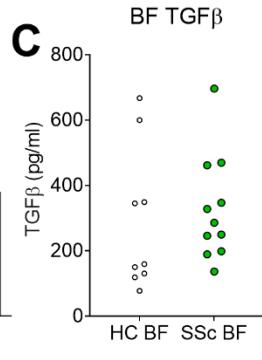
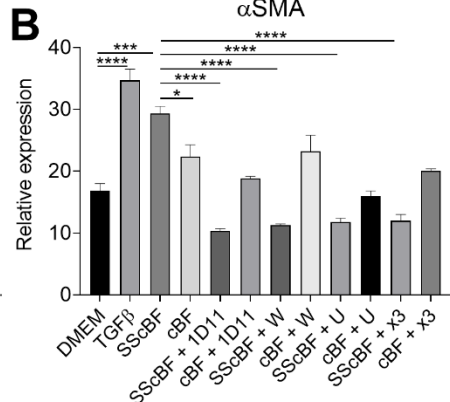
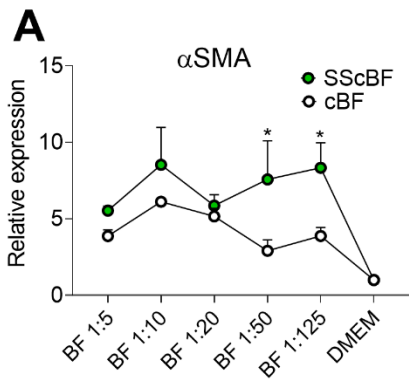
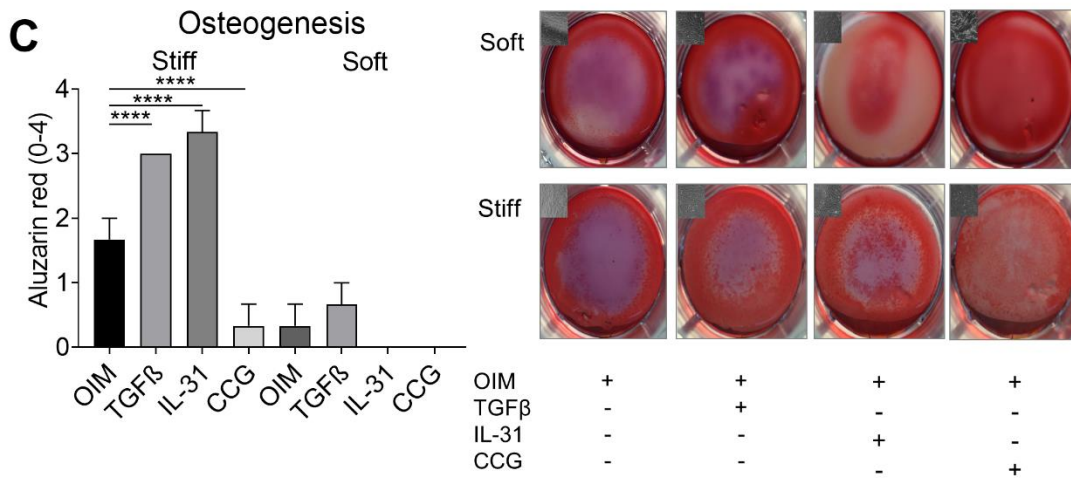
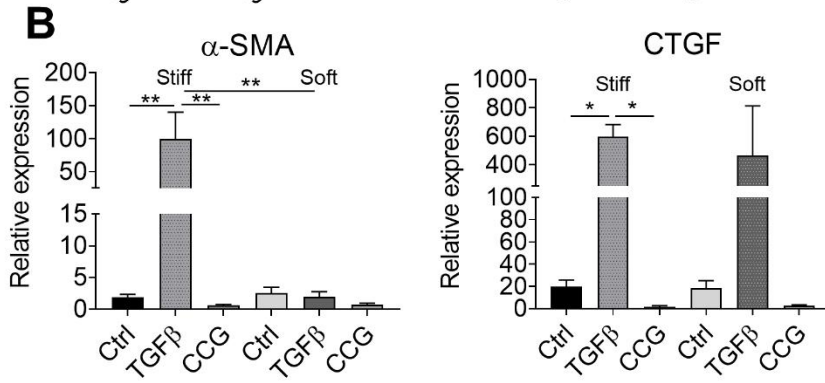
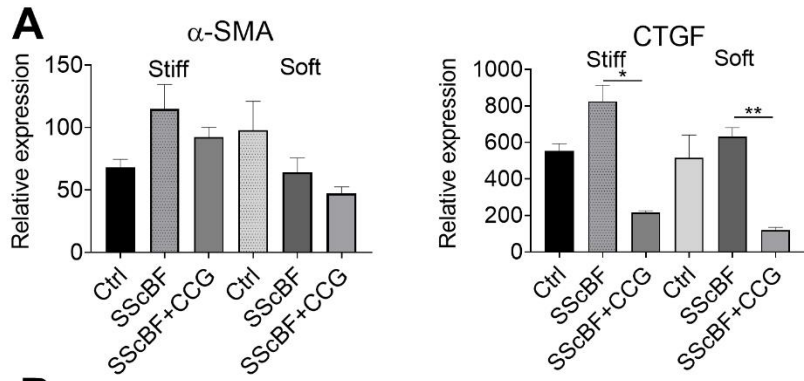


**Figure 4 Role of mechanical stress in MSC commitment in SSc** Modelling the tissue stiffness, soft 4 kPa or stiff 50kPa gels were used as ECM substrates for cultures of MSCs maintained with or without SSc BF or TGF $\beta$ . **(A)** Effect of SSc BF with or without the CCG mechanosensing inhibitor, on soft or stiff matrices on  $\alpha$ SMA and CTGF by qPCR. **(B)** Effect of tissue stiffness on TGF $\beta$  (4 ng/ml) induction of  $\alpha$ SMA and CTGF in MSCs. Both  $\alpha$ -SM and CTGF were suppressed by CCG1423 (10 $\mu$ M), indicating dependence on MRTF-A signal transduction. **(C)** MSCs cultured under osteogenic conditions on soft and stiff gels, effect of adding TGF $\beta$  or IL-31 and showing the effect of CCG1423 on osteogenic differentiation. (OIM=osteogenesis inducing medium, \*=p<0.05, \*\*=p<0.01, \*\*\*=p<0.001, \*\*\*\*=p<0.0001).



**Author contribution** ZT performed cell culture experiments and wrote the manuscript, EG and WT developed the metakaryotic staining method and performed the histologic studies. BY performed experiments with IL-31, HL performed cytokine assays of blister fluid. MM, ZH, NA,SV and YS collected dermal blister fluid from patients and controls, performed ELISA assays for TGF $\beta$ , IL-31 and lactate, revised the relevant sections of the manuscript and reviewed the final version, and performed tissue culture experiments , BAA performed tissue culture experiments, HL performed additional tissue culture experiments and Western blotting, added the relevant section of the manuscript concerning these protein assays and reviewed the final version of the manuscript, GT and AH performed osteogenic differentiation assays, GT performed osteogenic assays and additional GO analysis, added this data and reviewed the final version of the manuscript, CD contributed clinical data and reviewed the manuscript, CV performed and analyzed NGS studies, SOR performed lactate cell biology studies, SX performed cell biology experiments, RS conceived of the study, reviewed all data and co-wrote the manuscript.

**Acknowledgements** This study was supported by grants from Scleroderma Research UK, The Rosetrees' Trust, The Royal Free Charity, and Versus Arthritis.